

## Waddling and somersault motion of an adsorbed polymer in external fields

This article has been downloaded from IOPscience. Please scroll down to see the full text article.

2011 EPL 93 18002

(<http://iopscience.iop.org/0295-5075/93/1/18002>)

View [the table of contents for this issue](#), or go to the [journal homepage](#) for more

Download details:

IP Address: 134.99.64.185

The article was downloaded on 04/03/2011 at 07:40

Please note that [terms and conditions apply](#).

# Waddling and somersault motion of an adsorbed polymer in external fields

G.-L. HE<sup>(a)</sup>, R. MESSINA and H. LÖWEN

*Institut für Theoretische Physik II, Heinrich-Heine-Universität - Düsseldorf Universitätsstrasse 1, D-40225 Düsseldorf, Germany*

received 20 October 2010; accepted in final form 22 December 2010

published online 31 January 2011

PACS 83.10.Mj – Molecular dynamics, Brownian dynamics

PACS 83.50.Ax – Steady shear flows, viscometric flow

PACS 82.35.Gh – Polymers on surfaces, adhesion

**Abstract** – The dynamics of an adsorbed polymer chain along the substrate is studied using Brownian dynamics computer simulations of a bead-spring model. The polymer is end-functionalized and exposed both to a linear shear flow and an external field oscillatory in time which couples oppositely to the end beads and acts normal to the substrate. Different propagation modes are identified including a waddling-like and somersault-like polymer motion.

Copyright © EPLA, 2011

Stimuli-responsive polymers possess a wealth of possible applications, *e.g.* in biomedicine [1,2] and catalysis [3]. In particular, end-functionalized polymers are ideal since the respective ends can be addressed by external fields which makes it possible to stretch the polymer chain at wish—a key ingredient for micro-electronics [4] and micro-optics [5]. There is an increasing amount of activity in the synthesis and preparation of end-functionalized (or telechelic) polymers [6–8]. Moreover, computer simulations have revealed their dynamical response [9–13]. End-functionalized polymers in shear flow have been considered as well [14–17] but there are only few studies of adsorbed end-functionalized polymers under shear flow [18,19] which is mandatory in polymer transport, *e.g.* in micro-fluidic devices [20].

In this letter, we put forward the idea to steer the transport of adsorbed end-functionalized polymers by a combination of adsorption, shear flow and an additional external field. The external field which is the crucial ingredient in our study, is assumed to oscillate in time, to couple oppositely to the two end beads and to act perpendicular to the substrate. If the end groups are oppositely charged and the chain itself is neutral, an AC electric field provides a suitable realization of this external coupling.

Here we demonstrate, by extensive Brownian dynamics (BD) computer simulations of a bead-spring model, that the combination of shear, adsorption and external field

can induce different propagation modes of the polymer along the substrate. For an adsorbed chain, we identify a *waddling-like motion* for large external forces at small shear rates. Conversely, for small external forces and large shear rates, the polymer exhibits a *somersault-like motion*. If the external field is extremely large, the polymer lifts from the substrate and the bulk mode is characterized by *rolling and drifting*. The latter reduces to an oscillatory stretching mode in the absence of shear. We characterize these modes by monitoring the dynamics of the end-to-end distance and discuss the propagation speed of the chain along the substrate. Finally, possible experimental verifications and applications of these new modes are discussed.

The polymer chain is modelled as a series of  $N = 48$  coarse-grained spring beads. The adsorption is taken into account via a strong attraction from the substrate which is located at  $z = 0$ , defining the  $(x, y)$ -plane. The completely overdamped Langevin equations of motion for the positions  $\mathbf{r}_i(t) = (x_i(t), y_i(t), z_i(t))$  of bead  $i$  read as

$$\mathbf{r}_i(t + \delta t) = \mathbf{r}_i(t) + \frac{D_0}{k_B T} \mathbf{F}_i^{(tot)} \delta t + \delta \mathbf{G}_i + \dot{\gamma} z_i(t) \delta t \mathbf{e}_x \quad (1)$$

$$(i = 1, 2, \dots, N),$$

with the shear flow being in the  $x$ -direction ( $\mathbf{e}_x$  denoting the corresponding unit vector) and  $\dot{\gamma}$  denoting the shear rate. The shear gradient direction is along the vertical  $z$ -direction (see fig. 1). The thermal energy is denoted with  $k_B T$ . The Gaussian stochastic displacements  $\delta \mathbf{G}_i$  mimic

<sup>(a)</sup>E-mail: guili@thphy.uni-duesseldorf.de

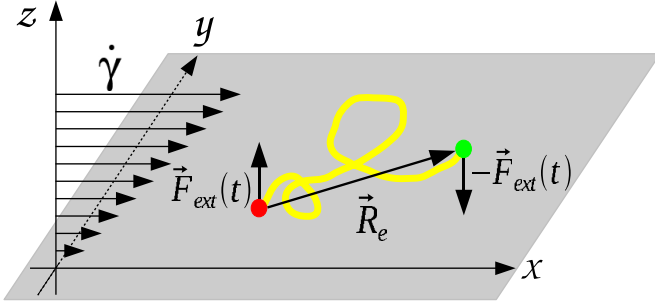


Fig. 1: (Colour on-line) Schematic representation of the setup and the coordinate system used. The substrate (grey plane) normal is along the  $z$ -direction and the shear flow as illustrated by velocity flow vectors is along the  $x$ -direction. The end beads of the functionalized polymer feel an opposite force of strength  $F$  along the  $z$ -direction, see also eq. (2). The end-to-end distance vector of the polymer chain is denoted by  $\vec{R}_e = (X_e, Y_e, Z_e)$ .

the collisions of the beads with the solvent molecules and assume a zero mean and a variance  $2D_0\delta t$  for each Cartesian component, with  $D_0$  denoting the free diffusion constant.

The total force  $\mathbf{F}_i^{(tot)}$  entering into eq. (1) has three contributions for the non-end beads ( $i = 2, 3, \dots, N-1$ ) [21,22]: i) bead-bead steric effects (repulsive interactions) are taken into account via a truncated and shifted purely repulsive Lennard-Jones potential  $U_{LJ}(r) = 4\epsilon[(\sigma/r)^{12} - (\sigma/r)^6 - (\sigma/r_c)^{12} + (\sigma/r_c)^6]$  with a cut-off at its minimum  $r_c = 2^{1/6}\sigma$ . Here,  $\epsilon = k_B T$  and  $\sigma$  (being the bead diameter) set the energy and length units, respectively, and  $r$  denotes the bead separation. ii) The “spring” is modeled via a finite extensible nonlinear elastic (FENE) [23] potential  $U_{FENE}(r) = -0.5KR_0^2 \ln[1 - (r/R_0)^2]$  which ensures the connectivity between adjacent beads along the backbone. We have set the spring constant to  $K = 27\epsilon/\sigma^2$ , and FENE cut-off to  $R_0 = 1.5\sigma$  which allows for a maximum bond length. iii) The adsorption at the substrate is mimicked by a Van-der-Waals-like strongly attractive potential  $U_A(z) = -A_0\epsilon(\sigma/z)^6$  with  $A_0 = 5$ . Besides, a repulsive stabilizing Lennard-Jones potential  $U_{LJ}(z) = 4\epsilon[(\sigma/z)^{12} - (\sigma/z)^6 - (\sigma/z_c)^{12} + (\sigma/z_c)^6]$  with  $z_c = 2^{1/6}\sigma$  is added, such that, the total wall potential employed here is  $U_W(z) = U_A(z) + U_{LJ}(z)$ .

The two functionalized end beads ( $i = 1$  and  $i = N$ ), on the other hand, experience an opposite additional force in the  $z$ -direction (see fig. 1), which is periodic in time and acts on the first bead as follows:

$$\mathbf{F}_{ext}(t) = \begin{cases} F\mathbf{e}_z & \left(0 \leq t < \frac{T_0}{2}\right), \\ -F\mathbf{e}_z & \left(\frac{T_0}{2} \leq t < T_0\right), \end{cases} \quad (2)$$

with  $\mathbf{e}_z$  being the unit vector in the  $z$ -direction and  $F$  is a force amplitude. The opposite force  $-\mathbf{F}_{ext}(t)$  is acting on the other end bead. The Brownian dynamics time step

used in the simulations is  $\delta t = 2 \times 10^{-6}\tau$ , where  $\tau = \sigma^2/D_0$  sets the time unit. Typically,  $10^9$  BD time steps are carried out for data production.

We have considered five different shear rates  $\dot{\gamma}\tau = 0, 1, 10, 50, 80$ , and five external force amplitudes  $F \cdot \sigma/\epsilon = 0, 1, 10, 100, 1000$  with three periods  $T_0/\tau = 6, 20, 40$  at fixed adsorption strength. Figure 2 shows an overview of the typical *cyclic* polymer chain motions in five relevant situations at  $T_0/\tau = 6$ . These observed modes are the result of the competition between four driving forces: i) adsorption, ii) bead thermal fluctuations, iii) shear which tends to transport lifted beads away into the flow direction and iv) the oscillatory external field which oscillatorily lifts and lowers the end beads. More explicitly, we have, see also fig. 2:

1. *Pulling*: No flow  $\dot{\gamma}\tau = 0$ , moderate external force  $F \cdot \sigma/\epsilon = 10$ : due to the strong adsorption and the weak external force, the polymer chain is not fully lifted/desorbed from the substrate in the regime of low period (see fig. 2(a)). The remaining part of the chain corresponds to a quasi-two-dimensional coil diffusing laterally on the substrate (top view not shown).
2. *Oscillatory stretching*: No flow  $\dot{\gamma}\tau = 0$ , strong external force  $F \cdot \sigma/\epsilon = 1000$ : the polymer chain is fully stretched perpendicular to the substrate and released from it<sup>1</sup> by the strong oscillatory external forces imposed on the ends (fig. 2(b)).
3. *Waddling*: Weak shear flow  $\dot{\gamma}\tau = 1$ , moderate external force  $F \cdot \sigma/\epsilon = 10$ : due to both weak shear flow and moderate external force, the chain behaves essentially like a coil in the large center part, and it follows the pull of the external force at the ends. Once an end is pulled up, it will be kicked by the flow with higher velocity there which makes it advance relatively to the lower adsorbed end (see fig. 2(c)). Thereby, over cycles, the ends are “waddling” and the rest of the chain is merely dragged forward in the direction of the flow. This is reminiscent to a waddling motion of a duck.
4. *Rolling + drifting*: Weak shear flow  $\dot{\gamma}\tau = 1$ , strong external force  $F \cdot \sigma/\epsilon = 1000$ : the strong external force lifts the chain from the substrate and stretches it considerably, and the weak shear flow makes it slightly inclined with respect to the normal  $z$ -direction (see fig. 2(d)). Just after the switch (*i.e.* at a half-cycle) of the force couple direction, the chain forms intermediate “S” shapes before exhibiting a monotonic shape profile. At this stage (after the transient “S” shapes), the chain will slightly roll (keeping its stretched form) under the effect of the shear flow.

<sup>1</sup>Note that the desorption of the chain occurs before the achievement of the cyclic motion. More precisely it is at the first switches of the external force that the chain release sets in.

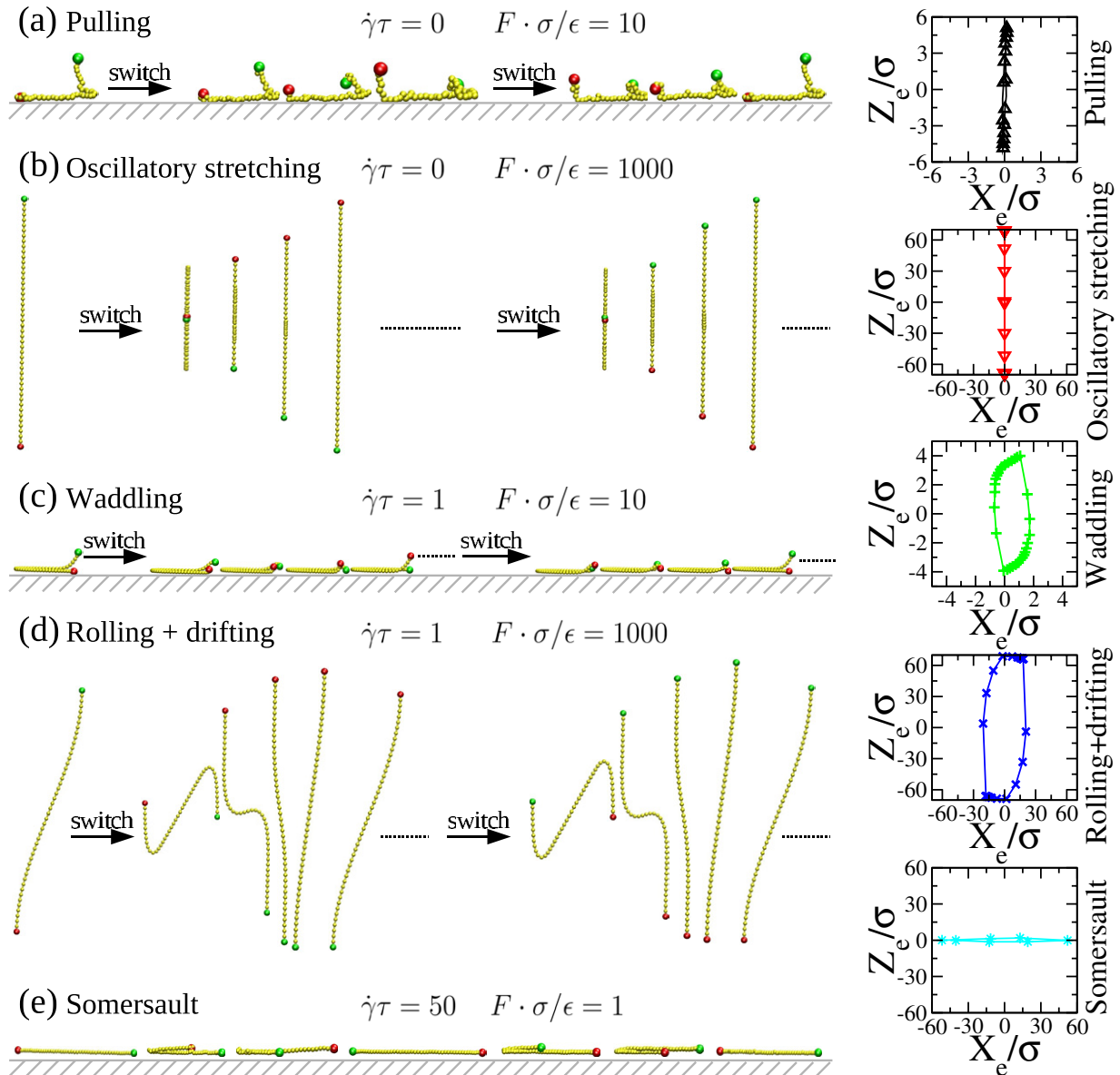


Fig. 2: (Colour on-line) Typical polymer chain motion (in an  $xz$  cross-sectional view) for five situations: (a) pulling,  $\dot{\gamma}\tau = 0$ ,  $F \cdot \sigma/\epsilon = 10$ : two end beads of the chain are pulled oscillatorily by the vertical external force field. Due to the strong adsorption at the substrate and the moderate external force, the central part of the chain is just fluctuating laterally in the  $xy$ -plane. (b) Oscillatory stretching,  $\dot{\gamma}\tau = 0$ ,  $F \cdot \sigma/\epsilon = 1000$ : due to the strong oscillatory external force, the chain is oscillatorily fully stretched and released from the substrate. (c) Waddling,  $\dot{\gamma}\tau = 1$ ,  $F \cdot \sigma/\epsilon = 10$ : because of the moderate oscillatory external force and the weak shear, the chain is waddling in the two ends along the flow on the substrate, and the rest part is just dragged forward. (d) Rolling and drifting,  $\dot{\gamma}\tau = 1$ ,  $F \cdot \sigma/\epsilon = 1000$ : the chain is extended and pulled out of the substrate by the strong oscillatory external force. Meanwhile, due to the flow velocity profile, it starts to roll at the time of switching force, and then when it reaches its steady states, it will be just drifting. (e) Somersault,  $\dot{\gamma}\tau = 50$ ,  $F \cdot \sigma/\epsilon = 1$ : due to the dominance of the strong shear (external force is weak here), the chain is more stretched in the flow direction. The somersault motion is a result from four contributions: the adsorption, the vertical external force, the bead thermal fluctuations, and the linear flow. The period of the external force for all five cases is  $T_0/\tau = 6$ . In addition to the snapshots the Lissajous plot of the  $x$  and  $z$  component of the end-to-end vector of the polymer chain,  $X_e$  and  $Z_e$ , respectively, are shown for the different types of modes.

5. *Somersault motion*: Strong shear flow  $\dot{\gamma}\tau = 50$ , quite small external force  $F \cdot \sigma/\epsilon = 1$ : due to the dominance of the strong shear (external force is weak here), the chain is more stretched in the flow direction. The

polymer motion is resulting from four effects: i) the adsorption, ii) thermal fluctuations, iii) the external periodic force and iv) the linear flow. Basically the mechanisms of motion in the present regime can be

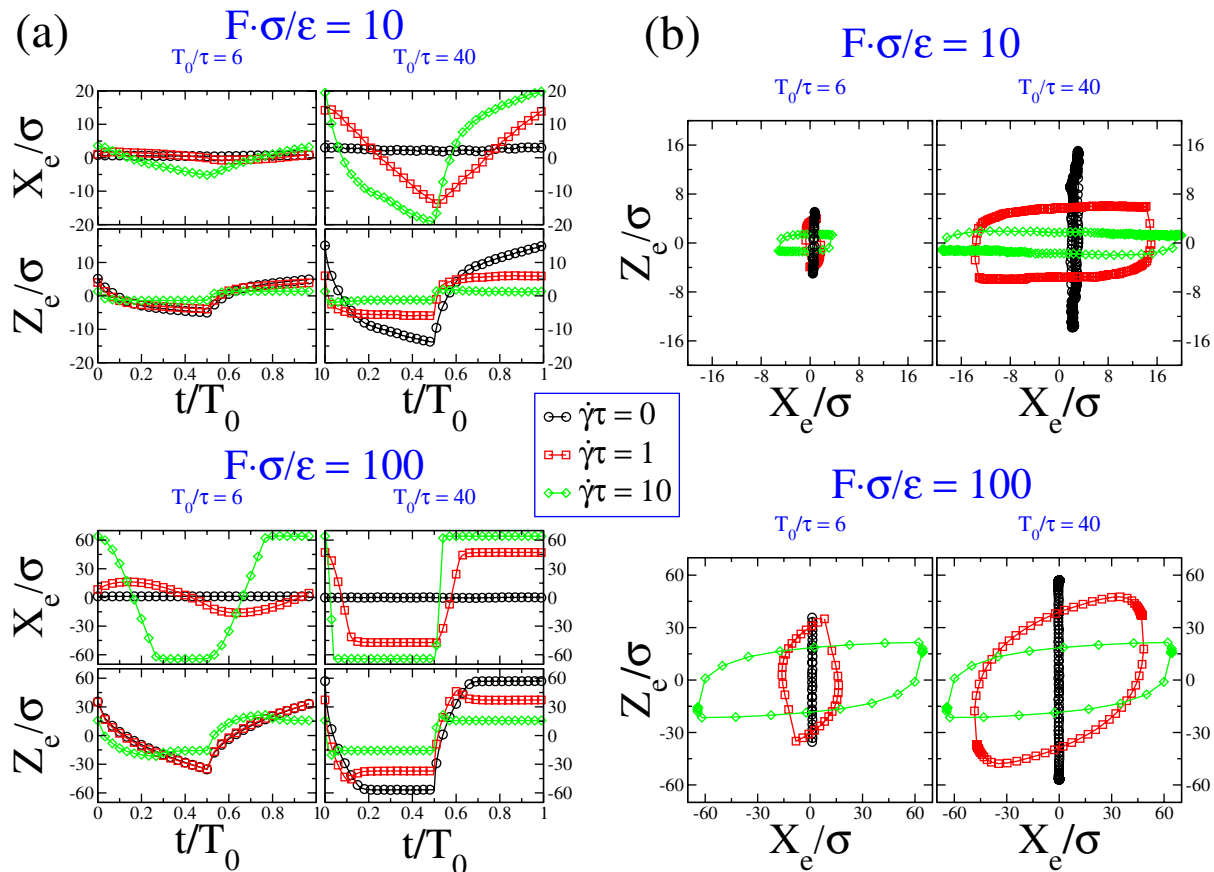


Fig. 3: (Colour on-line) (a) Two components of the chain end-to-end vector,  $X_e/\sigma$  and  $Z_e/\sigma$ , in the flow and vorticity direction as a function of time. (b) The locus of the vector  $\mathbf{R}_e/\sigma$  in the  $xz$ -plane. In (a) and (b), the plots are for the data at three shear rates  $\dot{\gamma}\tau = 0$  ( $\circ$ )  $\dot{\gamma}\tau = 1$  ( $\square$ )  $\dot{\gamma}\tau = 10$  ( $\diamond$ ), and under two external forces  $F \cdot \sigma/\epsilon = 10, 100$  in two periods  $T_0/\tau = 6, 40$ .

drawn as follows<sup>2</sup>. The adsorption and the attractive component of the external applied force contribute to the pivot move around the lower end. Then, the combined effect of i) the repulsive component of vertical external force, ii) the thermal fluctuations which make the polymer chain feels the inhomogeneity of the velocity field, promotes this somersault motion.

The five different types of motion can be distinguished more precisely as follows: first of all, oscillatory stretching and rolling+drifting occur as limiting cases in the bulk (in the absence of a substrate) whereas for pulling, waddling and somersault motion the substrate plays an essential role. Second, pulling and oscillatory stretching are limiting situations in the absence of shear. Qualitatively the

<sup>2</sup>Whereas both types of motion (waddling and somersault) involve a relative (cyclic) motion of the two ends along the flow direction, the amplitude of the step (*i.e.*, the largest end-to-end distance,  $X_e$ , in the flow direction) is quite different in each mode and correspond to typical length scales. For waddling, the step amplitude is about the order of a bead size. On the other hand, for the somersault motion the step amplitude is of the order of the chain size. These features are clearly evidenced in the corresponding Lissajous curves.

modes can further be distinguished by the motion of the end-to-end vector  $\mathbf{R}_e(t) = (X_e(t), Y_e(t), Z_e(t))$  of the polymer chain along one cycle. This can conveniently be plotted in a Lissajous-presentation, *i.e.* in trajectories in the  $(X_e Z_e)$ -plane. The corresponding averaged trajectories are also given in fig. 2. While in the absence of shear the loops are inflection symmetric with respect to  $X_e \rightarrow -X_e$ , this symmetry is broken under shear. Pulling and oscillatory stretching are strongly different in their extension  $Z_e$  in  $z$ -direction (compare the two scales for  $Z_e$  in the Lissajous plots). Rolling and drifting, on the other hand, is represented by an open loop involving long chain extensions, while waddling on the substrate is characterized by much smaller end-to-end distances. Finally, for somersault motion the chain extension in the vertical direction is strongly reduced due to the strong shear leading to a strong anisotropy in the loop.

While the different modes discussed above were obtained for extreme parameter combinations, intermediate situations will lead to modes between these limiting cases. This is illustrated in fig. 3 for less extreme external forces and two different periods  $T_0$ . What is shown here are the components  $X_e(t)$  and  $Z_e(t)$  of the end-to-end

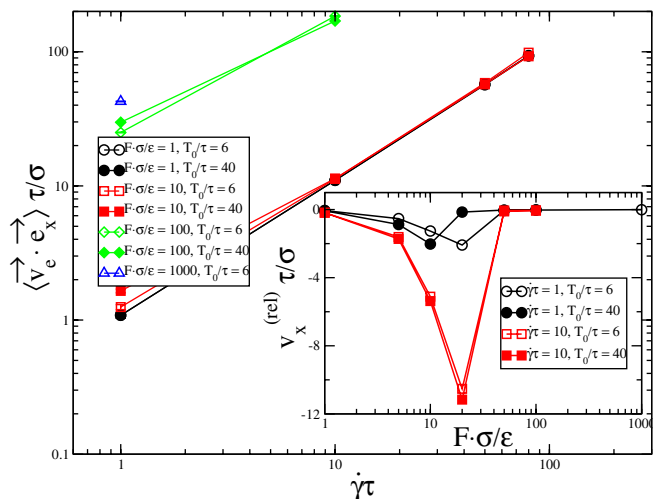


Fig. 4: (Colour on-line) Averaged velocity of the chain end in the flow ( $x$ -) direction  $\langle \mathbf{v}_e \cdot \mathbf{e}_x \rangle \tau / \sigma$  as a function of the reduced shear rate  $\dot{\gamma} \tau$ . Inset: velocity  $v_x^{(rel)} \tau / \sigma$  relative to the shear flow of an end bead as a function of the reduced external force  $F \cdot \sigma / \epsilon$ .

vector as a function of time  $t$  and the corresponding Lissajous plot in the  $(X_e, Z_e)$ -plane. The data monitor the evolution of the end-to-end distance along one cycle and were obtained by a statistical average over typically 100 subsequent cycles. Clearly, the maximal extension in  $z$ -direction is always decreasing with growing shear rates, reflecting the fact that shear tends to align and stretch the chain along the flow direction, (see fig. 3(a)). Concomitantly, the maximal extension in  $x$ -direction is always increasing with growing shear rates, at prescribed external force (see fig. 3(a)). Moreover, at prescribed shear rate, the maximal extension in  $z$ -direction is increasing with  $F$ . In the regime of strong external forces (here  $F \cdot \sigma / \epsilon = 100$ ),  $Z_e$  does not behave monotonically (within a half-period), see fig. 3(a), as a non-trivial result of the competition between shear-induced  $x$ -alignment and external force-induced  $z$ -alignment. The corresponding Lissajous plots in fig. 3(b) reveal similar loop behaviour as discussed before (see fig. 2). However, the force and shear rate parameters considered in fig. 3 include intermediate regimes where the polymer motion can be more complicated than those advocated in fig. 2.

Moreover, we studied the propagation speed of the polymer chain along the substrate by monitoring the averaged velocity of one chain end in the  $x$ -direction, *i.e.* by plotting the  $x$ -component ( $\langle \mathbf{v}_e \cdot \mathbf{e}_x \rangle$ ) of the chain end velocity. At prescribed shear rate, this quantity is growing with increasing external force, see fig. 4, since the (upper) end is influenced more strongly by the flow due to its higher height. However, the absolute velocity  $\langle \mathbf{v}_e \cdot \mathbf{e}_x \rangle$  is mainly dictated by the shear flow profile itself. This explains the roughly unit slope in the double logarithmic plot in fig. 4. More subtle deviations are revealed in the relative velocity,  $v_x^{(rel)} = \langle \mathbf{v}_e \cdot \mathbf{e}_x \rangle - v_{lf}$ , where  $v_{lf} = \dot{\gamma} h$  is

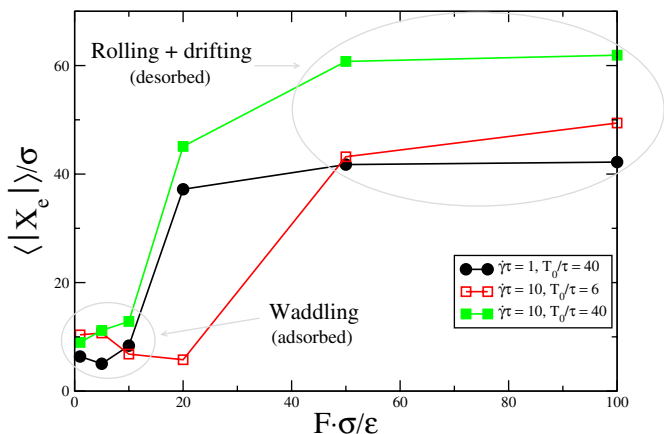


Fig. 5: (Colour on-line) Average reduced end-to-end distance amplitude  $\langle |X_e| \rangle$  in the flow direction as a function of the amplitude of the reduced external force  $F \cdot \sigma / \epsilon$  for different reduced shear rates  $\dot{\gamma} \tau$ .

the flow velocity at the time-averaged height of the chain end  $h$ . Interestingly, this relative velocity is found to be non-monotonic with the external force (see the inset in fig. 4). This is explained as follows: the vertical fluctuations of the chain end are not very different from the rest of the beads under weak external force. Hence, the entire chain just flows close to the substrate with a corresponding (very) low velocity. When the external force is quite strong, the whole chain (firstly) desorbs and is strongly stretched, as illustrated in fig. 2(d). Consequently, the chain drifts roughly according to the flow velocity profile leading to a (very) small value of  $v_x^{(rel)}$ . In the case of intermediate external forces, one part of the chain is adsorbed (as illustrated on fig. 2(c)) and drifts with low velocity accordingly. The other part of the chain that is pulled up is dragged by the flow. Nonetheless, it is the slow adsorbed part of the chain that governs the overall velocity of the chain and therefore leads to a “retardation” compared to the flow due to the adsorption and the chain connectivity.

As a last result, we explore the behaviour of the end-to-end distance in the flow direction  $|X_e|$  at prescribed reduced low shear rates. The results can be found in fig. 5. Thereby, one can clearly distinguish two regimes, namely: i) waddling (appearing at low reduced external force) which is characterized by an extension  $|X_e|$  roughly of the order of the bead size; and ii) “rolling + drifting” (appearing at high reduced external force), which is of the order of the chain size, see fig. 5. Notice that these two regimes correspond also to adsorbed and desorbed situations respectively.

In conclusion, we have shown that combined external fields, such as shear flow and a time-oscillating force-field coupling, to end-functionalized adsorbed polymers can lead to novel complex dynamical modes of propagation. Two different types of modes correspond to a waddling-like and a somersault-like motion. The propagation speed of the polymer exposed to these fields can be steered

by the relative amplitude of the applied fields. The findings can be exploited to control polymer motion along flat or nanopatterned substrates [24]. For example, the periodic somersault motion can be efficiently used to induce polymers jump over steric obstacles on the substrate resulting in a possible device which separates different kinds of polymers as they respond differently to the external fields. An experimental verification of the dynamics predicted here is possible by studying adsorbed polymers under shear [21] which have oppositely charged endgroups and are exposed to an external electric field [25].

A future study should analyze the interesting and non-trivial interplay between the frequency of the imposed external force and that of the polymer tumbling [26,27]. Hydrodynamic interactions were neglected and especially the resulting lift. Nonetheless, since the adsorption under consideration is (very) strong, this effect should not be truly relevant thereby. However, a future more complete analysis would be indicated to quantitatively account for hydrodynamic interactions.

\*\*\*

We thank M. STAMM for helpful discussions. This work was supported by the DFG within the SFB TR6 (project D1).

#### REFERENCES

- [1] NAPOLI A., VALENTINI M., TIRELLI N., MÜLLER M. and HUBBELL J. A., *Nat. Mater.*, **3** (2004) 183.
- [2] YORK A. W., KIRKLAND S. E. and MCCORMICK C. L., *Adv. Drug Deliv. Rev.*, **60** (2008) 1018.
- [3] DAI S., RAVI P. and TAM K., *Soft Matter*, **5** (2009) 2513.
- [4] TUCCITTO N., FERRI V., CAVAZZINI M., QUICI S., ZHAVNERKO G., LICCIARDELLO A. and RAMPI M. A., *Nat. Mater.*, **8** (2009) 41.
- [5] ARPIAINEN S., JONSSON F., DEKKER J. R., KOCHER G., KHUNSIN W., TORRES C. M. S. and AHOPELTO J., *J. Adv. Funct. Mater.*, **19** (2009) 1247.
- [6] BAEK J.-B., QIN H., MATHER P. T. and TAN L.-S., *Macromolecules*, **35** (2010) 4951.
- [7] WONG E. H. H., STENZEL M. H., JUNKERS T. and BARNER-KOWOLLIK C., *Macromolecules*, **43** (2010) 3785.
- [8] KAMADA J., KOYNOV K., CORTEN C., JUHARI A., YOON J. A., URBAN M. W., BALAZS A. C. and MATYJASZEWSKI K., *Macromolecules*, **43** (2010) 4133.
- [9] MALVALDI M., ALLEGRA G., CIARDELLI F. and RAOS G., *J. Phys. Chem. B*, **109** (2005) 18117.
- [10] PHILLIPS C. L., IACOVELLA C. R. and GLOTZER S. C., *Soft Matter*, **6** (2010) 1693.
- [11] QIAO R. and BRINSON L. C., *Compos. Sci. Technol.*, **69** (2009) 491.
- [12] ROY S., MARKOVA D., KUMAR A., KLAPPER M. and MÜLLER-PLATHE F., *Macromolecules*, **42** (2009) 841.
- [13] KLOS J. S. and SOMMER J.-U., *Macromolecules*, **43** (2010) 4418.
- [14] MANIAS E., CHEN H., KRISHNAMOORTI R., GENZER J., KRAMER E. J. and GIANNELIS E. P., *Macromolecules*, **33** (2000) 7955.
- [15] ZHENG Q., XIA D., XUE Q., YAN K., GAO X. and LI Q., *Appl. Surface Sci.*, **255** (2009) 3534.
- [16] SPRAKEL J., SPRUIJT E., STUART M. A. C., BESSELING N. A. M., LETTINGA M. P. and VAN DER GUCHT J., *Soft Matter*, **4** (2008) 1696.
- [17] KOGA T. and TANAKA F., *Macromolecules*, **43** (2010) 3052.
- [18] CHESTAKOVA A., LAU W. and KUMACHEVA E., *Macromolecules*, **37** (2004) 5047.
- [19] MENG X. X. and RUSSEL W. B., *J. Rheol.*, **50** (2006) 169.
- [20] KOSTER S., STEINHAUSER D. and PFOHL T., *J. Phys.: Condens. Matter*, **17** (2005) S4091.
- [21] HE G.-L., MESSINA R., LÖWEN H., KIRIY A., BOCHAROVA V. and STAMM M., *Soft Matter*, **5** (2009) 3014.
- [22] HE G.-L., MESSINA R. and LÖWEN H., *J. Chem. Phys.*, **132** (2010) 124903.
- [23] KREMER K. and GREST G. S., *J. Chem. Phys.*, **92** (1990) 5057.
- [24] LI B., FANG X. H., LUO H. B., SEO Y. S., PETERSEN E., JI Y., RAFAILOVICH M., SOKOLOV J., GERSAPPE D. and CHU B., *Anal. Chem.*, **78** (2006) 4743.
- [25] STAMM M., private communication.
- [26] SCHROEDER C. M., TEIXEIRA R. E., SHAQFEH E. S. G. and CHU S., *Phys. Rev. Lett.*, **95** (2005) 018301.
- [27] KOBAYASHI H. and YAMAMOTO R., *Phys. Rev. E*, **81** (2010) 041807.